Solar Energy 224 (2021) 35–42

Contents lists available at ScienceDirect

Solar Energy

journal homepage: www.elsevier.com/locate/solener

Polar solar power plants – Investigating the potential and the design challenges

Iver Frimannslund [a,*], Thomas Thiis [a], Arne Aalberg [b], Bjørn Thorud [c]

[a] Norwegian University of Life Sciences, Department of Building- and Environmental Technology, NO-1432 Ås, Norway
[b] University Centre in Svalbard, Department of Arctic Technology, NO-9171 Longyearbyen, Svalbard and Jan Mayen
[c] Multiconsult ASA, Department of Solar, Smart-grid and Storage, NO-0276 Oslo, Norway

ARTICLE INFO

Keywords:
Snow
Energy yield
Bifacial
Module temperature
Snowdrifts
Snow fence

ABSTRACT

The potential for power production and the climatic effects imposed on ground mounted solar power plants in Polar climates are scarcely documented and limit the use of solar power in Polar regions. The study investigates the potential and the design challenges of Polar solar power plants through field measurements of a small-scale solar power plant with modules facing both sky and ground in Adventdalen, Svalbard. The climate is characterized by significant horizontal redistribution of snow due to little shelter and strong winds, causing snowdrifts to develop in the aerodynamic shade of the PV arrays. In this study we show that snowdrifts pose a significant challenge for solar power plants in Polar climates as they can grow to cover the plant, resulting in reduced power production and an imposed mechanical load on the PV arrays. The snowdrifts produced by the PV arrays exhibit a similarity with that produced by porous snow fences and it is argued that snow fence theory can be applied to PV arrays to control the accumulation. The results from solar power production indicates that the module yield is enhanced by the low temperatures as a seasonal performance ratio of 92.5% in combination with below-STC backsheet temperatures are measured. The bifacial gain displays a strong seasonal variation due to the presence snow cover and averages 14.7% annually. The findings indicate that the Polar climate enhance the module performance and that an adaption of solar power plant design is necessary for the system to be resilient to snowdrift development.

1. Introduction

In the past, the use large-scale solar power plants have been limited to climates defined by an abundance of irradiance often referred to as the "Sunbelt" (Wang, 2019). As the prices for solar power have decreased, solar power is becoming competitive also at higher latitudes. The dispersion of large-scale solar power plants has continued past the Sunbelt, and in the future, the decrease of solar power price is expected to continue, potentially further increasing the competitiveness of the technology (ITRPV, 2020).

The competitiveness of solar power at higher latitudes is not only hinged upon decreased production costs, but also at the performance of solar modules due to the characteristics of high latitude climates. A favourable characteristic is the influence of temperature on solar cell efficiency (Duffie & Beckman, 2013). A decrease in cell temperature increases the solar cell voltage and slightly decreases the current, but the net outcome is an increased power output of approximately 0.35–0.5% per kelvin. The performance ratio describes the power output of a solar system compared to the power produced in Standard Test Conditions (STC) and is a measure of the efficiency of the system. In general it is found that the performance ratio increases with latitude due to the influence of temperature dependency on solar cells (Bayrakci et al., 2014).

Additionally, the reflected irradiance due to the high albedo of snow can increase the irradiance collected by a solar module. Bifacial solar modules produce power from the irradiance received on both sides of the module and can significantly increase the power output of solar modules in high-albedo climates (Guerrero-Lemus et al., 2016; Sun et al., 2017; Wittmer & Mermoud, 2018). To describe the net surplus of produced energy from a bifacial module, the bifacial gain (also referred to as "the gain efficiency product") is a factor calculated as the increased power output of a bifacial module compared to a monofacial module with the same configuration (Guerrero-Lemus et al., 2016). Schmid and Reise (2015) used numerical simulations to investigate the bifacial gain for various configuration and albedo values and found a variation from 5 to 24% annually. The combination of low temperatures and ground reflected irradiance increases the performance of solar power

* Corresponding author.

https://doi.org/10.1016/j.solener.2021.05.069
Received 7 December 2020; Received in revised form 21 May 2021; Accepted 23 May 2021
Available online 5 June 2021

normalized to the incoming global horizontal irradiance (Dubey et al., 2013; Sun et al., 2017; Wang, 2019).

Solar power production can thus be more effective in Polar regions and several studies also indicate that there is a market for solar power in the Arctic and the Antarctic. Polar settlements which rely on fossil fuels as the main energy supply are documented to have high fuel cost due to the transportation of the fuel to the remote settlements (Nazarova et al., 2019; Tin et al., 2010). The Russian Government has declared that the high dependence on imported fossil fuels, high energy intensity and high levelized cost of electricity are problematic areas of the development in the Arctic (Nazarova et al., 2019). Similarly, research stations in Antarctica experience the same challenges as fuel is commonly shipped by boat from the mainland and then by overland vehicles for inland stations (Tin et al., 2010). In a case study of a solar power plant "fuel saver" for the Troll research station in Antarctica, it was estimated that a solar power plant covering 50% of the consumption has a Return-On-Investment of 6 years due to a 50% reduction of the LCOE (S. Merlet, 2016). Reduced solar irradiation in the Polar regions as compared to the "Sunbelt" region is thus compensated by increased efficiency resulting from low temperatures and high albedo. The competitiveness of solar PV is further strengthened by the high fuel costs of the existing solutions.

The yield of PV systems in Polar regions is scarcely documented in scientific literature but a few examples document both measured and simulated performance. The yield should be compared carefully as it is strongly influenced by the configuration of the system as well as local shading conditions. In Antarctica, the Syowa station has 55 kW of ground mounted solar modules installed with a steep tilt and a 60° azimuth from true north both east and west with a reported specific yield of 800 kWh/kWp/year (Tin et al., 2010). In the Arctic, a specific yield of 621 kWh/kWp/year is reported for a 13.8 kW roof mounted system in Longyearbyen with a south-east azimuth and an approximate tilt of 20° (Svalbards Miljøvernfond, 2013). For the same location, Ringkjøb et al. (2020) simulated a specific yield of 672 kWh/kWp/year for a 30° south facing fixed tilt system. The simulations were performed using the Global Solar Energy Estimator (GSEE) simulation code (Pfenninger & Staffell, 2016) and MERRA-2 climate data (Gelaro et al., 2017).

The implementation of solar power systems to Polar regions must confront the climatic effects imposed by snow and ice. Snow on the modules is unfavorable as it shades the module surface resulting in a power generation loss and imposes a mechanical load on the module (Andenæs et al., 2018). An increased module tilt increases the probability of snow shedding and can reduce the snow shading losses and the snow load (Andrews et al., 2013; Granlund et al., 2019). Such studies are relevant for topographies less influenced by wind where the snow cover is dominated by vertical precipitation but are not necessarily applicable to windy, unsheltered areas dominated by horizontal redistribution of snow. The Polar tundra and Polar ice-cap climate from Köppen Geiger climate classification (Kottek et al., 2006) commonly have little vegetation to shelter from the wind, and little precipitation as well (Grzegorz, 2010). Although the annual precipitation is typically low in Polar regions, the horizontal snow-flux due to the combination of exposed terrain and high wind speeds can be large in magnitude (Mellor, 1965). The redistribution of snow is caused by snow eroding from exposed areas and accumulating in sheltered areas, creating snowdrifts. The formation of snowdrifts can be considered as a direct consequence of the aerodynamic shade from objects or terrain where the shear stress on the snow particles is reduced below a threshold limit (Thiis & Ferreira, 2014). To reduce snowdrifts in unwanted areas, the design of infrastructure in Polar regions is commonly adapted to control where snow is deposited and eroded (Thiis & Gjessing, 1999; Tominaga, 2018). Snow fences can be implemented as a measure to retain the snow in upwind accumulations zones.

In this study, it is argued that the theory of the properties of snow fences can be applied to ground mounted PV arrays. Tabler (2003) has extensively studied how the properties of snow fences influence the snowdrift shape and storage capacity. His findings include that the length and height of fully developed snowdrifts are approximately proportional to the fence height (Tabler, 1980a). This allows to use scaled models for investigating the snowdrifts produced by larger snow fences (Tabler, 1980b). Further he showed that the inclination of snow fences has the effect of displacing the nose of the snowdrift and changing both length and storage capacity (Tabler, 2003). An inclination leaning with the wind displaces the nose of the drift upwind and increases length and the storage capacity while an inclination into the wind produces the opposite result as wind is forced underneath the snow fence. However, inclining the snow fence reduces the fence height which has the effect of reducing the storage capacity. Similarly, the bottom gap of snow fences influences the storage capacity as well. A bottom gap of 10–15% of the total height of the fence is considered optimal, while increasing the gap beyond this height reduces the depth and storage capacity of the drifts

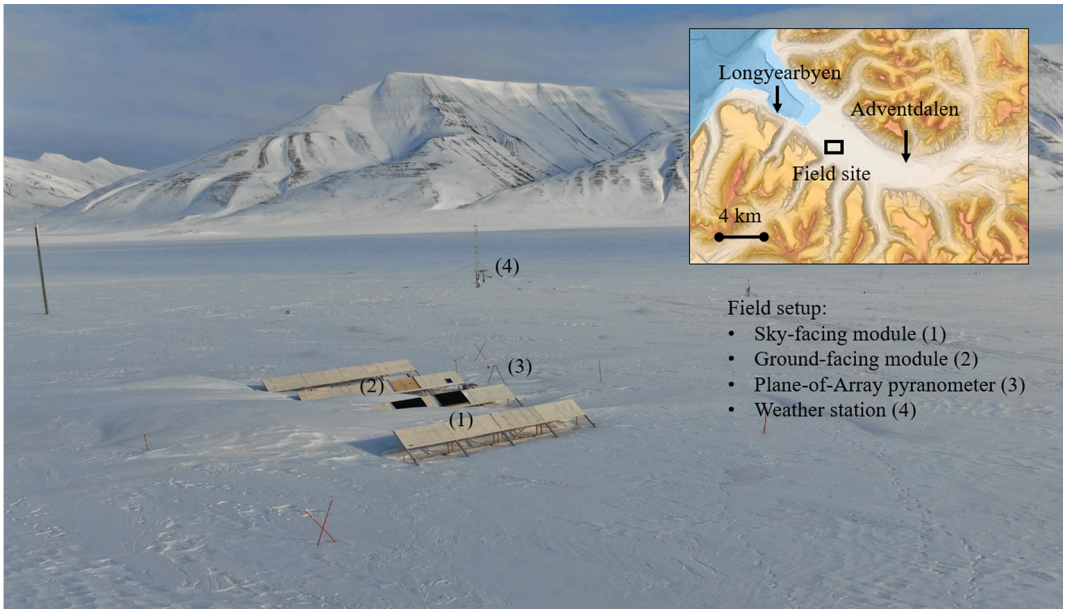

Fig. 1. Field setup and site location. Four 10 m long PV mock-up rows are placed at the valley floor in Adventdalen. PV modules are mounted on the rows and a weather station and a Plane-of-Array pyranometer are installed in proximity to the setup.

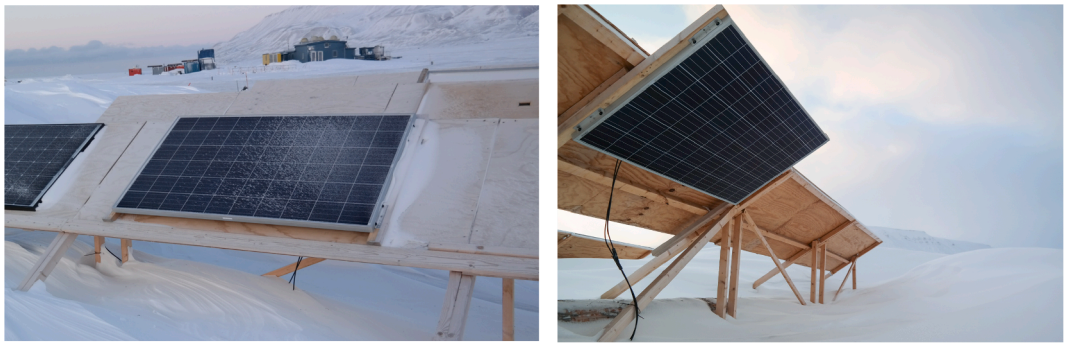

Fig. 2. Module installation with a sky-facing module (left) and a ground-facing module (right). The modules are lifted 2 cm from the wooden surface to allow for ventilation on the backside.

and displaces the nose of the drift further downwind. The profile of a snowdrift measured parallel to the wind is independent of incident wind directions (referred to as "attack angles" by Tabler) between 45 and 90° in relation to the longitudinal alignment of the fence (Tabler, 1980a). However, the cross-section area and length of the snowdrift vary with wind direction and can be expressed as the sine of the attack angle multiplied by the cross-section area or length formed by a wind direction perpendicular to the snow fence (Tabler, 2003). These properties of snow fences are connected to the properties of PV arrays and are discussed in Section 4.

For redistribution of snow in solar power systems the existing research mostly concern the influence of solar power system on roof snow loads. Ferreira et al. (2019) used wind tunnel experiments and numerical simulation to study the friction velocity on a roof surface with solar panel arrays and found that the arrays differentiate the friction velocity at roof surfaces and that the bottom gap and wind direction in relation to the system azimuth is determinative for the accumulation conditions. Brooks et al. (2014) and Grammou et al. (2019) used water flume simulations to investigate aerodynamical drift patterns on low tilt roof mounted systems and found that the drift patterns were influenced by the presence of the arrays.

This study investigates the power production potential and the climatic effects imposed on a small-scale ground mounted mock-up solar power plant in the Adventdalen valley in Svalbard. The climate in the valley is characterized by low precipitation (213 mm annually on average) and strong winds from a uniform direction (Gallet et al., 2019). The upwind distance capable of transporting snow (fetch) is large enough so that the horizontal snow flux is only limited by the evaporation of the wind-blown snow (Tabler, 2003). Several snowdrift studies have previously been performed at the same location (Jaedicke, 2001; Thiis & Gjessing, 1999). As the latitude of the site is 78° North, the seasonal variations in solar irradiance are significant. Midnight sun and wintertime darkness each occur for approximately four months of the year, with a transition between the two extremes of only two months. At summer solstice, the solar altitude is 35.2° midday (south), and 11.8° at midnight (north).

2. Field measurement setup

The investigated solar power plant in this study is a fixed tilt system constituting of four mock-up rows made of 2x3″ spruce beams and plywood with solar modules mounted on top as shown in Fig. 1. This section presents the specification of the field measurement setup.

2.1. PV design layout

Established principles of PV plant design are used to determine the configuration of the arrays. The system has a south facing azimuth to maximize the yield. Although the optimal tilt to maximize received solar irradiance in a collector plane is 50°, an angle of 30° was chosen to increase the ground cover ratio. Simulations with PVsyst indicate a 5% irradiance reduction by adjusting the tilt from 50° to 30° (PVsyst SA, 2020). The rows are spaced to avoid interrow shading for a solar altitude higher than 10°, resulting in a pitch of 5.5 m. The total height of the system is 1.3 m and the effective bottom gap between array and ground is approximately 0.65 m. Solid timber poles (length = 12 m, diameter = 20–30 cm) are used as ballast for the arrays to secure for high wind speeds. The beams are partially covered by snow and ice in wintertime. The gross surface of each array is 1.2x10 m, allowing for standard sized module (1x1.6 m) to be placed in landscape orientation.

2.2. PV modules and inverter

Two monofacial modules are installed on the 30° wooden rack in opposite directions as shown in Fig. 2: one facing the sky and one facing the ground. A bifacial module was installed as well but was covered by the snowdrifts during the beginning of the production season and suffered significant power production losses. Both monofacial modules are installed at the middle rows to provide similar shading conditions. The ground-facing module is elevated slightly above the mock-up arrays to

Table 1
Snowdrift measurement data. Days of snowdrift development represent the number of days in the field with a potential of snow redistribution, with the first day of such conditions estimated to be the 1st of October. H is the height of the system and is equal to 1.3 m.

Event	Date	Days of snowdrift development	Drift length / H	Maximum snow depth / H	Volume [m^3]
Installation	12.03.19	0	–	–	–
Measurement 1	21.03.19	12	17	0.53	34.3
Measurement 2	10.05.19	60	22	0.58	130.6
Measurement 3	21.02.20	143	45	1.27	778.8
Measurement 4	07.04.20	189	50	1.38	1007.6

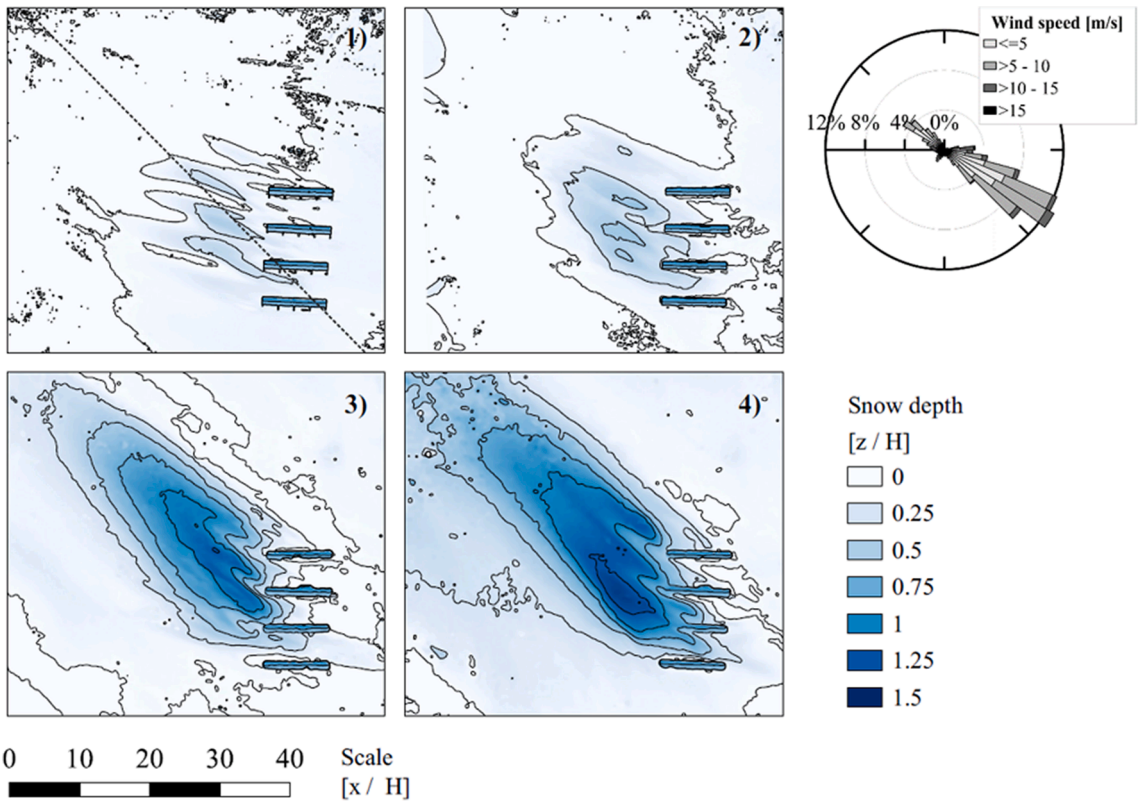

Fig. 3. Map displaying the snow depth for measurement 1–4. The wind rose in the upper right corner displays the wind conditions at the site. The dashed line in measurement 1 marks a cross-section of the snowdrifts displayed in Fig. 4.

reduce the effect of shading from the rack. The distance from the ground to the bottom of the panel is approximately 1.0 m. Plane-of-Array irradiance (POA) and reflected Plane-of-Array irradiance (POA_r) are logged with a pyranometer outside of the plant. Additionally, a backsheet temperature sensor was installed on the sky-facing module. To measure the power produced by the modules, current and voltage of each module are logged with a sample rate of 10 s with a Campbell Scientific CR1000X datalogger. The voltage and current are measured on the DC-side from the inverter.

The monofacial modules are of the type JKM265P by Jinko Solar with a rated performance of 265 W_p at STC. The inverter and built-in MPPT is the CI-Mini-1200H from CyboEnergy (CyboEnergy, 2020). The inverter is made for off-grid purposes and produces variable AC-voltage for heating elements. As the site offers no grid connection possibilities, the inverter is suitable for the setup as the load from the modules is consumed on-site by heating cables. The inverter displayed a variable capability to accurately detect the MPP of the modules. To compensate for the variability of the inverter, the results were filtered to obtain the maximum value in 2-minute intervals. The same filtration on the irradiance data increases the annual Plane-of-Array irradiance less than 5%. In general, snow was not removed from the modules throughout the season. However, the modules were cleaned after soiling events caused by a nearby road.

3. Results

3.1. Solar power plant snowdrifts

Short time after the installation of the solar power plant in the field, snowdrifts were observed in the leeward side of the plant. To document the development of the snowdrifts, photogrammetry was used to construct 3D models of the snowdrifts at different timesteps. A total of four measurements were performed over two winters. The snow drifts melted entirely between the winters. Table 1 shows key numbers from the measurements, while Fig. 3 virtually display the snowdrift depth for all four measurements. The results are presented in relation to the total

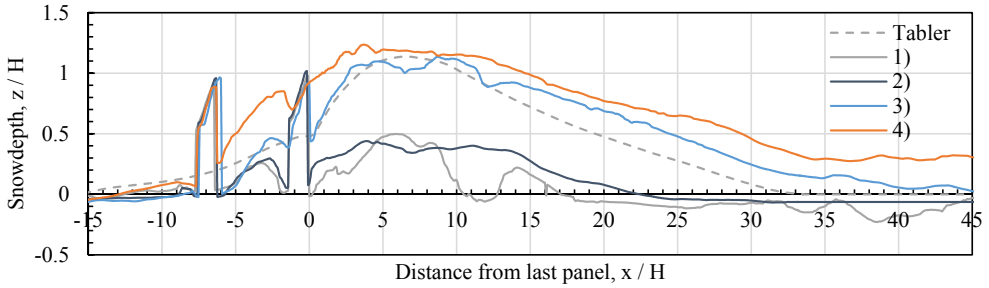

Fig. 4. Snowdrift height and length in relation to the PV height for measurement 1–4. The dashed line marks equilibrium drifts from a 3.8 m tall 50% porous snow fence (Tabler, 1989).

Fig. 5. An aerial photography displays the scale of the snowdrifts at measurement 3.

height of the array (equal to 1.3 m).

The results show an increase of drift length, height and volume with the time of exposure in the field. The accumulation mainly occurs at the leeward side of the PV arrays corresponding to the prevailing wind direction. On measurement 3 and 4, the height of the drifts exceeds the height of the arrays. In measurement 4, the snowdrifts extend onto the arrays and close the gap for the second southernmost array.

A cross-section parallel to the prevailing wind direction (indicated by the dashed line in Fig. 3) is displayed in Fig. 4. The cross section of the snowdrifts produced by the PV arrays is compared with the cross section of snowdrifts produced by a 3.8 m tall 50% porous snow fence. Fig. 4 shows that the snowdrifts from the PV arrays exhibit a similarity with snowdrifts from the snow fence.

To provide a better sense of scale to the drifts, an aerial photography from measurement 3 shows the size of the drifts in relation to passing snow-mobile transport in Fig. 5.

Table 2
Module yield for the monofacial sky- and ground-facing modules. A theoretical bifacial yield with 80% bifaciality factor is calculated from the monofacial modules yield. The bifacial gain is calculated as the relative difference in production to the sky-facing module.

Module	Annual production [kWh]	Specific yield [kWh/kWp/year]	Performance ratio* [%]	Bifacial gain [%]
Mono. sky	177.6	670.0	92.5	–
Mono. ground	32.6	122.9	–	–
Bifacial	203.7	768.3	–	14.7

* The performance ratio is calculated in an interval from July to October due to an error with the Plane-Of-Array pyranometer.

3.2. Solar power production

Solar power production began in 5th of March and ended the 19th of October. A few days at the very beginning of the season was missed due to a malfunction of the logging system. However, the influence on the total production is small due to weak irradiance in the early season. The annual yield of the system is shown in Table 2. A theoretical bifacial yield is calculated as the sum of the yield of the sky-facing module and 80% of the ground-facing module. It thus represents a bifacial module with an 80% Bifaciality factor (Guerrero-Lemus et al., 2016).

Irradiance measurements from the nearby weather stations show that the irradiance in 2020 was 7.9% lower than the annual average from the last 5 years of complete irradiance datasets. If the yield is scaled proportional to the irradiance, a long-term average specific yield of 727.8 and 834.6 kWh/kWp/year is obtained for the sky-facing module and the bifacial module respectively.

The performance of the ground-facing module in relation to the sky-facing module displays a strong seasonal variation due to the seasonal variations in snow cover and irradiance. Fig. 6 shows the seasonal variation of the relative performance.

Here it can be seen that the relative performance of the ground-

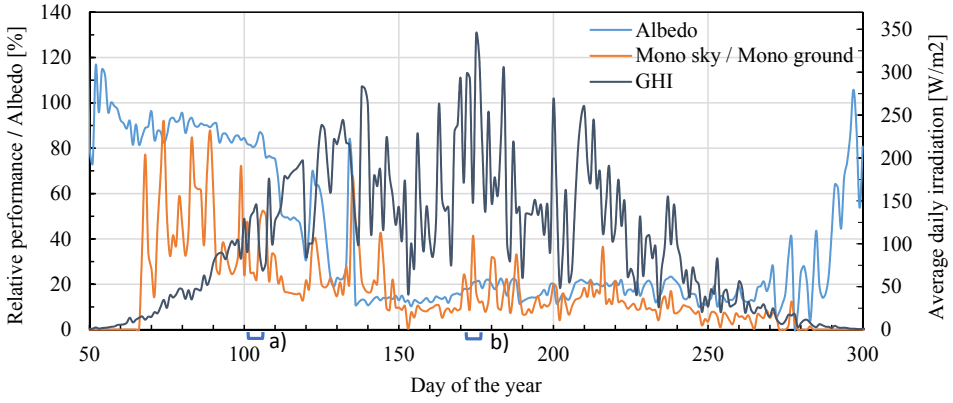

Fig. 6. Relative performance of the ground-facing module in relation to the sky-facing module compared with albedo and global horizontal irradiance. The graph is produced with daily average data.

Table 3
Seasonal variations in the production of the sky- and ground-facing module in relation to the presence of the snow cover.

Snow cover status	Production monofacial-sky [Wh/day]	Production monofacial-ground [Wh/day]	Sky-facing module / Ground-facing module [%]
During snow cover	525.0	196.2	37.4
After snow cover	828.8	129.0	15.6

facing module is reduced around day 110 due to the melting of the snow cover. The performance of the modules in relation to the presence of the snow cover is quantified in Table 3.. Here it can be seen that the production of the ground-facing module is higher before the melting of snow cover although the incoming global horizontal irradiance is weaker. Daily production profiles from three consecutive days in summer and spring in Fig. 7 illustrates this phenomenon. In spring, the performance of the bifacial module is increased by a significant contribution of rear-side irradiance and reach the same production peak as in summer although the global horizontal irradiance is weaker. In summer, the contribution from the ground reflected irradiance is less and makes up a small part of the total power production. However, the bifacial module has a secondary production peak at midnight due to irradiance on the backside of the module. The midnight production is not only caused by ground-reflected irradiance, but from direct irradiance from the north as well. This phenomenon enables uninterrupted power production in summer.

The backsheet temperature of the monofacial sky-facing module was logged during the entire year. Fig. 8 shows a scatterplot of the backsheet temperature in relation to the module yield. A trend of increasing temperature with increasing yield is evident, as is expected due to the heat produced from the PV module during operation. Most of the power production occur well below STC-temperature.

4. Discussion

The development of snowdrifts in a solar power plant is an undesired phenomenon that can limit power production and impose a mechanical load on the PV arrays. The solar power plant investigated in this study was designed with established principles of solar power plant design commonly used at lower latitudes and resulted in a development of snowdrifts in the Adventdalen climate. The accumulation was severe and partially buried one array towards the end of the second winter. The constant development of the snowdrifts during the measurements indicates that no equilibrium state of the snowdrifts is achieved, and that the accumulation is likely to continue. This is also likely for the fourth measurement where the gap beneath one of the PV arrays is closed by the snowdrift. The closing of the gap changes the flow field and is likely to prolong the accumulation and a potential equilibrium-state snowdrift. The results suggest that for a solar power plant to be sustainable in Polar

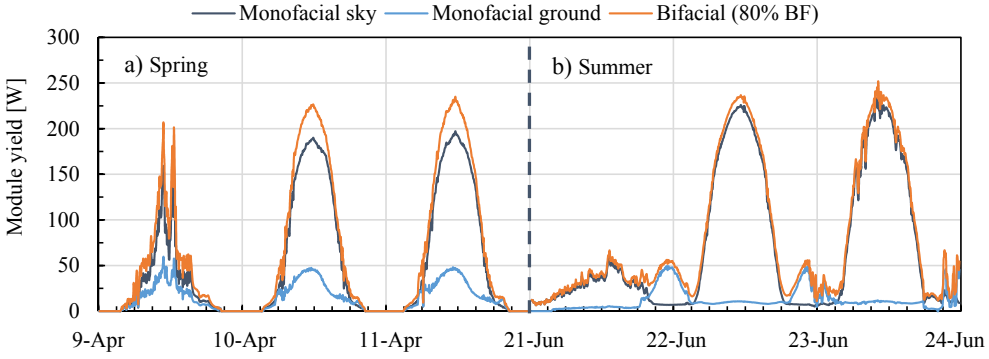

Fig. 7. Production profiles from three consecutive days for the monofacial sky-facing module, monofacial downward-facing module and a theoretical bifacial module with an 80% bifaciality factor.

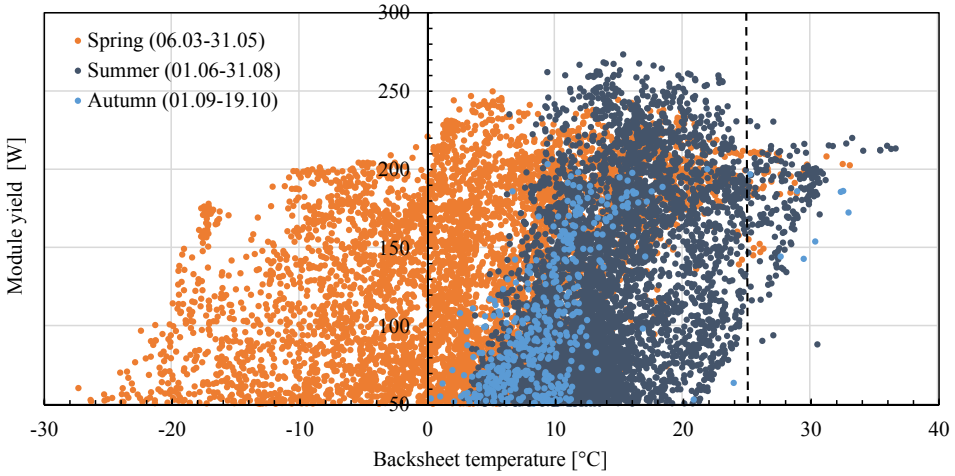

Fig. 8. Backsheet temperature in relation to the yield of the monofacial sky-facing panel from 5-minute average data. The dashed line marks the STC-module temperature.

regions, the plant should be adapted to be resilient against snowdrift development.

As snowdrifts are a direct consequence of the aerodynamic shade from objects and terrain, a modification of the design of the solar power plant can be used to control snow accumulation and erosion in the plant. In this study, the snowdrifts produced from the PV arrays exhibit a strong similarity with snowdrifts produced by porous snow fences. The development of the snowdrifts viewed as a cross-section parallel to the wind direction, shown in Fig. 4, is very similar to experimental studies on snow fences performed by Tabler (2003). The similarity indicates that snow fence theory can be applied to PV arrays and used to control snowdrift accumulation in solar power plants. The design can be adapted so that snow is deposited in designated areas (as with snow fences) or so that the deposition is minimized. How to adapt snow fences to maximize snow deposition is thoroughly documented in research, but how similar structures can be adapted to minimize the accumulation is seldom investigated and is the topic of the discussion to follow.

Several findings from snow fence studies can be connected to the properties of solar power plants. As the snow drift cross section area and length decrease with the sine of the wind direction (where 90° is perpendicular) (Tabler, 2003), an attack angle parallel to PV arrays is favourable to reduce snow accumulation. Shifting the azimuth of the plant can thus be used to reduce snow accumulation in climates with uniform wind directions such as in Adventdalen. However, the influence of the rack itself should be taken into account in such cases. The finding also indicates that if the attack angle in the field measurement setup was 90° instead of 30-45°, the length and cross section area of the snowdrifts could increase by up to 50%. The empirical expression from Tabler is valid for single snow fences, but it could be argued that the effect on several consecutive PV arrays would only propagate the accumulation.

The effect of snow fence inclination and bottom gap on snow drifts documented by Tabler (2003) can also be applied to the PV arrays. A strong inclination of snow fences reduces the net height of the fence and the resulting snow storage capacity. Strongly inclining the PV arrays while maintaining a bottom gap is therefore likely to reduce the storage capacity of the PV produced snow drifts. An empirical expression from Tabler (1994) shows that the relationship of the bottom gap and total height should be equal to 0.75 to avoid any snow storage. For the configuration of the power plant in Adventdalen, this implies that the gap between the array and the ground should be equal to 1.8 m. This is almost three times the gap as used in the field measurement setup. For a single array, this expression is likely conservative as it does not take into account the inclination of the array. However, the effect of several consecutive arrays can have an adverse effect on the accumulation conditions.

The knowledge from snow fence design indicates that the azimuth, array tilt and bottom gap of PV arrays can be adjusted to minimize snow accumulation in the plant. Additionally, the distance between the arrays is likely to influence the accumulation. The properties discussed here are likely applicable to PV arrays of varying size as the snowdrifts produced by snow fences are approximately proportional to the height of a snow fence (Tabler, 1980b). Scaling the PV array properties (including the array surface, the distance between arrays and the bottom gap) will, therefore, likely produce a similar result as shown in this study.

Changing the configuration of the plant will influence yield and costs of the system. The design of ground mounted solar power plants in climates with high snow redistribution should balance between designing a system with high energy yield and a system is optimized for snowdrift accumulation. The latter is necessary to provide a climate robust system ensuring the long-term sustainability of the system. The challenge lies in optimizing for two very different design criteria where an optimization of one can have an unfavorable effect on the other.

A specific yield of 670 and 768.3 kWh/kWp/year was measured for the sky-facing module and a theoretical bifacial module respectively. However, the irradiance in 2020 was 7.9% lower than average and indicates that the measured specific yield is likely underestimated compared with a long-term average. If the yield is scaled proportional to the irradiance, a long-term average specific yield of 727.8 and 834.6 kWh/kWp/year is obtained. Scaling the yield proportional with the irradiance does not consider the effect of increased module temperature and may slightly overestimate the module yield. Ringkjøb et al. (2020) reported a specific yield of 672 kWh/kWp/year for a monofacial module with numerical simulations of a system with the same configuration and same location as in the field measurements. However, the irradiance used in the numerical simulations was 11.9% higher than the measured irradiance at the field site in 2020. The discrepancies between simulated and measured yield may arise from differences in system specifications or from inaccurate estimation of the module performance.

A performance ratio of 92.5% was measured between July and October for the sky-facing module. As mentioned, the performance ratio is the performance of the system in the field compared to the performance at STC and is influenced by the system quality, module temperature, shading conditions and other factors. Performance ratios above 90% is considered high and signifies a well-performing system (Reich et al., 2012). The measured backsheet temperature shown in Fig. 8 indicates that the cell temperature is well below STC-temperature for the majority of the season. The measured backsheet temperature data supports that low cell temperature is likely to have a strong influence on the measured performance ratio. As the performance ratio in this study is only calculated from July-October and measured temperatures are the lowest in spring, an all-year performance ratio is likely to exceed the reported performance ratio. It is important to note that the produced power is logged on the DC-side and therefore does not take into account the conversion efficiency of the inverter.

A bifacial gain of 14.7% was calculated for a theoretical bifacial module with 80% bifaciality factor. The bifaciality factor is commonly in the range of 60–95% (Tian Shen et al., 2019). The simplification of taking the sum of the production of two monofacial modules does not take into account the non-symmetrical layout of a bifacial cell or the effect of double side glazing on the optical losses and temperature (Halm et al., 2014; Hubner et al., 1997; Janssen et al., 2017). Additionally, the ground-facing module only received irradiance on the front side of the module (facing the ground) which contributes to artificially low module temperatures during operation. However, the measured bifacial gain of 14.7% is high and encourages the use of bifacial modules in Polar regions. As the bifacial gain is a system specific property that is influenced by configuration and albedo, a higher bifacial gain can be achieved for climates with a higher average albedo or for designs with a more favourable configuration than the case investigated.

Polar ice cap climates are defined by the warmest average monthly temperature not exceeding 0 °C (Kottek et al., 2006). In such climates, the snow cover is constant, providing a high albedo the entire power production season. With a bifacial solar power system configured to utilize the reflected irradiance in combination with a climate contributing to low cell temperatures, the efficiency of a solar power system can potentially be higher than any place on earth. However, if snowdrifts develop in the system, they will not melt. The presence of snow over consecutive years theoretically signifies the formation of a glacier. The potential benefits of Polar solar power plants can therefore be high but preconditions a system resilient to snowdrift development.

5. Conclusion

The small-scale power plant in Adventdalen produced snowdrifts jeopardizing the functionality of the system. To ensure the resilience of solar power plants in snow drift climates, the design should be adapted to snowdrift development. This can be performed by adapting the configuration of the PV arrays so that snow is deposited in designated areas or so that the deposition is minimized. In this study, it is found that snowdrifts produced by the PV arrays exhibit a strong similarity with snowdrifts produced by snow fences. The similarity indicate that principles of snow fence design can be applied to PV arrays. Research on

snow fence theory imply that several properties of the PV arrays can be adjusted to control the snow accumulation. The properties which can be adjusted includes the azimuth of the plant, the tilt of the arrays and the gap between the array and the ground. In addition, the effect of several consecutive PV arrays must also be accounted for. The results from PV power production show a specific yield of 670 kWh/kWp/year for the sky-facing module but may not be representative of a long-term average due to annual variations in irradiance. The performance ratio is a metric normalized to the POA-irradiance and was measured at 92.5% for the sky-facing module. The logged backsheet temperature of the module indicates a positive contribution from low temperatures. The climate is favourable for bifacial power production due to a significant contribution from ground reflected irradiance. A theoretical bifacial yield is calculated from the yield of the monofacial modules, representing a bifacial module with 80% bifaciality factor. The bifacial gain is measured to be 14.7% and the contribution of rear side irradiance is shown to vary with the seasons due to the presence of the snow cover. The findings highlight the potential of solar power production in Polar climates as well as the design challenge due to snowdrift development from the system. An adaption of the design of solar power plants which ensures high yield and snowdrift resilience should be performed to enable the dispersion of ground mounted solar power plants to Polar regions.

Declaration of Competing Interest

The authors declare that they have no known competing financial interests or personal relationships that could have appeared to influence the work reported in this paper.

References

Andenæs, E., Jelle, B., Ramlo, K., Kolås, T., Selj, J., Foss, S., 2018. The influence of snow and ice coverage on the energy generation from photovoltaic solar cells. Sol. Energy 159, 318–328. https://doi.org/10.1016/j.solener.2017.10.078.

Andrews, R., Pollard, A., Pearce, J., 2013. The effects of snowfall on solar photovoltaic performance. Sol. Energy 92, 84–97. https://doi.org/10.1016/j.solener.2013.02.014.

Bayrakci, M., Choi, Y., Brownson, J.R.S., 2014. Temperature dependent power modeling of photovoltaics. Energy Procedia 57, 745–754. https://doi.org/10.1016/j.egypro.2014.10.282.

Brooks, A., Gamble, S., Dale, J., Gibbons, M., 2014. Determining Snow Loads on Buildings with Solar Arrays. International Structural Specialty Conference, Halifax, NS.

CyboEnergy, 2020. Available at: http://www.cyboenergy.com/ (accessed: 12.11.2020).

Dubey, S., Sarvaiya, J.N., Seshadri, B., 2013. Temperature dependent photovoltaic (PV) efficiency and its effect on PV production in the world – a review. Energy Procedia 33, 311–321. https://doi.org/10.1016/j.egypro.2013.05.072.

Duffie, J.A., Beckman, W.A., 2013. Design of photovoltaic systems. Solar Engineering of Thermal Processes. John Wiley & Sons Inc, Hoboken, New Jersey.

Ferreira, A., Thiis, T., A. Freire, N., M.C., Ferreira, A., 2019. A wind tunnel and numerical study on the surface friction distribution on a flat roof with solar panels. Environ. Fluid Mech., 19. doi: 10.1007/s10652-018-9641-5.

Gallet, J.-C., Björkman, M., Borstad, C., Hodson, A., Jacobi, H.W., Larose, C., Luks, B., Spolaor, A., Urazgildeeva, A., Zdanowicz, C., 2019. Snow research in Svalbard: current status and knowledge gaps.

Gelaro, R., McCarty, W., Suárez, M., Todling, R., Molod, A., Takacs, L., Randles, C., Darmenov, A., Bosilovich, M., Reichle, R., et al., 2017. The modern-era retrospective analysis for research and applications, version 2 (MERRA-2). J. Clim. 30 https://doi.org/10.1175/JCLI-D-16-0758.1.

Grammou, N., Pertermann, I., Puthli, R., 2019. Snow loads on flat roofs with elevated solar panel arrays. Steel Construction 12 (4), 364–371. https://doi.org/10.1002/stco.201900031.

Granlund, A., Narvesjö, J., Malou Petersson, A., 2019, 2019. The Influence of Module Tilt on Snow Shadowing of Frameless Bifacial Modules. 36th European Photovoltaic Solar Energy Conference and Exhibition, Marseille, September 9-13, 2019, pp. 1650-1654.

Grzegorz, R., 2010. Climate: Polar. In: Warf, B. (Ed.), Encyclopedio of Geography. SAGE Publications.

Guerrero-Lemus, R., Vega, R., Kim, T., Kimm, A., Shephard, L.E., 2016. Bifacial solar photovoltaics – A technology review. Renew. Sustain. Energy Rev. 60, 1533–1549. https://doi.org/10.1016/j.rser.2016.03.041.

Halm, A., Aulehla, S., Schneider, A., Mihailetchi, V., Roescu, R., Galbiati, G., Libal, J., Kopecek, R., 2014. Encapsulation losses for ribbon contacted N-type IBC solar cells. Proceedings of the 29th European Photovoltaic Solar Energy Conference and Exhibition.

Hubner, A., Aberle, A. & Hezel, R. (1997, 29 Sept.-3 Oct. 1997). Temperature behavior of monofacial and bifacial silicon solar cells. Conference Record of the Twenty Sixth IEEE Photovoltaic Specialists Conference - 1997.

ITRPV, 2020. International Technology Roadmap for Photovoltaic.

Jaedicke, C., 2001. Drifting snow and snow accumulation in complex terrain. University of Bergen.

Janssen, G.J.M., Tool, K.C.J., Kossen, E.J., Van Aken, B.B., Carr, A.J., Romijn, I.G., 2017. Aspects of bifacial cell efficiency. Energy Procedia 124, 76–83. https://doi.org/10.1016/j.egypro.2017.09.334.

Kottek, M., Grieser, J., Beck, C., Rudolf, B., Rubel, F., 2006. World Map of the Köppen-Geiger Climate Classification Updated. Meteorol. Z. 15, 259–263. https://doi.org/10.1127/0941-2948/2006/0130.

Mellor, M., 1965. Cold Regions Science and Engineering Part III, Section A3c. Hanover, New Hampshire.

Nazarova, Y., Sopilko, N., Kulakov, A., Shatalova, I., Myasnikova, O., Bondarchuk, N., 2019. Feasibility study of renewable energy deployment scenarios in remote arctic communities. Int. J. Energy Econ. Policy 9, 330–335. https://doi.org/10.32479/ijeep.7343.

Pfenninger, S., Staffell, I., 2016. Long-term patterns of European PV output using 30 years of validated hourly reanalysis and satellite data. Energy 114, 1251–1265. https://doi.org/10.1016/j.energy.2016.08.060.

PVsyst SA, 2020. PVsyst. route du Bois-de-Bay 107, Satigny, Switzerland.

Reich, N., Müller, B., Armbruster, A., van Sark, W., Kiefer, K., Reise, C., 2012. Performance ratio revisited: is PR > 90% realistic? Prog. Photovoltaics Res. Appl. 20, 717–726. https://doi.org/10.1002/pip.1219.

Ringkjøb, H.-K., Haugan, P.M., Nybø, A., 2020. Transitioning remote Arctic settlements to renewable energy systems – A modelling study of Longyearbyen, Svalbard. Appl. Energy 258, 114079. https://doi.org/10.1016/j.apenergy.2019.114079.

S. Merlet, T. T., B. Thorud, E. Olsen, J. Nyhus. (2016). Challenges of PV Generation in Polar Regions. Case Study: the Norwegian Research Station "Troll" in Antarctica. 32nd European Photovoltaic Solar Energy Conference and Exhibition.

Schmid, A., Reise, C., 2015. Realistic Yield Expectations for Bifacial PV Systems - An Assessment of Announced, Predicted and Observed Benefits. 31st European Photovoltaic Solar Energy Conference and Exhibition.

Sun, X., Khan, M., Deline, C., Alam, M., 2017. Optimization and performance of bifacial solar modules: a global perspective. Appl. Energy 212. https://doi.org/10.1016/j.apenergy.2017.12.041.

Svalbards Miljøvernfond, 2013. Sluttrapport - publikumsvennlig, 3/36 Bygningsintegrert solenergianlegg – Etablering i Elvesletta Syd.

Tabler, R.D., 1994. Design guidelines for the control of blowing and drifting snow. Strategic Highway Research Program.

Tabler, R.D., 2003. Controlling Blowing and Drifting Snow with Snow Fences and Road Design. Niwot, Colorado.

Tabler, R.D., 1980a. Geometry and density of drifts formed by snow fences. J. Glaciol. 26 (94), 405–419. https://doi.org/10.3189/S0022143000010935.

Tabler, R.D., 1980b. Self-similarity of wind profiles in blowing snow allows outdoor modeling. J. Glaciol. 26 (94), 421–434. https://doi.org/10.3189/S0022143000010947.

Tabler, R. D. (1989). Snow fence technology: State of the art. First International Conference on Snow Engineering, Santa Barbara, California.

Thiis, T., Ferreira, A., 2014. Sheltering effect and snow deposition in arrays of vertical pillars. Environ. Fluid Mech. 15 https://doi.org/10.1007/s10652-014-9356-1.

Thiis, T.K., Gjessing, Y., 1999. Large-scale measurements of snowdrifts around flat-roofed and single-pitch-roofed buildings. Cold Reg. Sci. Technol. 30 (1), 175–181. https://doi.org/10.1016/S0165-232X(99)00021-X.

Tian Shen, L., Pravettoni, M., Deline, C., Stein, J., Kopecek, R., Singh, J.P., Luo, W., Wang, Y., Aberle, A., Khoo, Y.S., 2019. A review of crystalline silicon bifacial photovoltaic performance characterisation and simulation. Energy Environ. Sci. 12 https://doi.org/10.1039/C8EE02184H.

Tin, T., Sovacool, B.K., Blake, D., Magill, P., El Naggar, S., Lidstrom, S., Ishizawa, K., Berte, J., 2010. Energy efficiency and renewable energy under extreme conditions: Case studies from Antarctica. Renewable Energy 35 (8), 1715–1723. https://doi.org/10.1016/j.renene.2009.10.020.

Tominaga, Y., 2018. Computational fluid dynamics simulation of snowdrift around buildings: Past achievements and future perspectives. Cold Reg. Sci. Technol. 150, 2–14. https://doi.org/10.1016/j.coldregions.2017.05.004.

Wang, Z., 2019. Chapter 2 - The Solar Resource and Meteorological Parameters. In: Wang, Z. (Ed.), Design of Solar Thermal Power Plants. Academic Press, pp. 47–115.

Wittmer, B., Mermoud, A., 2018. Yield Simulations for Horizontal Axis Trackers with Bifacial PV Modules in PVsyst. 35th European Photovoltaic Solar Energy Conference and Exhibition.